Beckmann, M.; Krüger, S.; Spiegel, W.: A Method for Non-Invasive Heat Flux Detection in Membrane Walls of Steam Generators. In: Proceedings of the International Conference on Incineration & Thermal Treatment Technologies - IT3, 15.05.–19.05.2006, Savannah (USA). ISBN 978-0-9232-0484-6

A METHOD FOR NON-INVASIVE HEAT FLUX DETECTION IN MEMBRANE WALLS OF STEAM GENERATORS

Beckmann, M., Krüger, S., Bauhaus-Universität Weimar,

Spiegel, W., CheMin GmbH Augsburg

1 INTRODUCTION

For the thermal treatment of wastes and recovery of energy from biomass the combustion-post combustion process with grate firing (conventional Municipal Solid Waste Incineration (MSWI) plants) have worked satisfactorily over many decades. However, the potential for advancements in this area has not yet been exhausted, and important objectives of the continuous development in MSWI-plants remain:

- increasing the plant efficiency,
- development and implementing primary measures for reducing pollutants,
- lowering flue gas mass flows,
- improving of ash quality,
- reducing of corrosion,
- longer availability period and
- enhancement of economic efficiency.

To prevent corrosion, knowledge concerning the formation of deposits (especially on steam generator surfaces) during operation is important.

The formation of a deposit (fouling layer) causes an additional heat resistance, i.e. the heat transfer within the boiler is reduced. An abrupt increase of the calorific value, caused by varying waste composition, can induce a short-time temperature rise. As a consequence, alkaline heavy metal compounds can be transported to super heater (convective) region.

During operation, with the help of the online heat flux measurement on the membrane walls, the formation of deposits (fouling layers), as well as the condition of the refractory lining, (changing of microstructure, defects etc.) can be determined. Therefore, for example, suitable intervals for the cleaning of the membrane walls can be specified by the operator more exactly and thus temperature shifts in the boiler with appropriate corrosion sequences within the super heater range can be avoided.

The theoretical background of the online heat flux measurement is described briefly in the first part of this paper. Next, the test facility for investigating membrane wall segments is presented, and the measuring technique is described. In addition, a comparison of results of the mathematical model with the experimental results is provided. Finally, first measurement results taken from on-site application on a membrane wall of a boiler are discussed.

2 THEORETICAL BACKGROUND OF THE ONLINE HEAT FLUX MEASUREMENT

As the physical background of the online heat flux measurement on membrane walls of steam generators was already described in detail in [1], it will only be described briefly here.

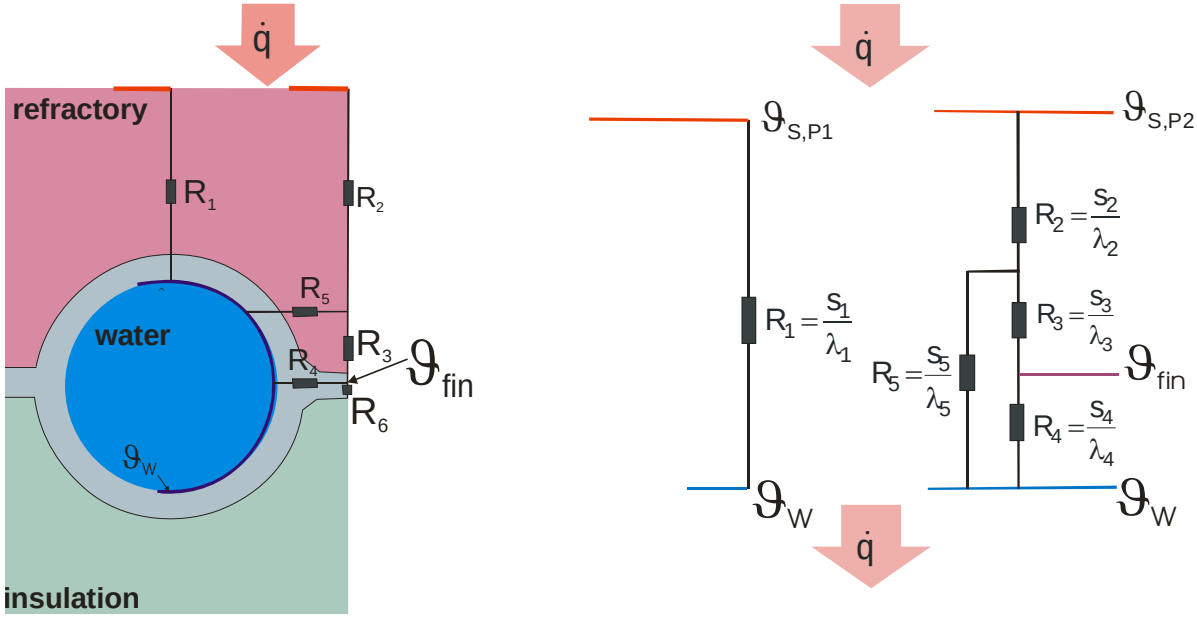

a) Alternate circuit diagram, close to reality.

b) Alternate circuit diagram, simplified.

Fig. 1. Construction of the wall – alternate circuit diagram.

Fig. 1 shows a wall construction with refractory lining, boiler tube and insulation. The incoming heat flux density (resulting from the combustion) – is transferred from the surface of the refractory lining to the boiling water only by conduction. The temperature of the boiling water in the tube is constant due to the vaporization pressure of the feed water system.

The heat flux density, which comes to the surface of the refractory lining in the region of the tube, can directly pass through the wall to the boiling water. The heat flux density, which comes to the surface of the refractory lining in the region of the fin, is only partially transferred to the boiling water in the region of the inner part of the tube (furnace-side) (represented by the R5 heat resistance in Fig. 1a and b). A further part of the heat flux density is transferred over the fin of the membrane wall to the boiling water (represented by the R4 heat resistance in Fig. 1a and b). Consequently, a horizontal heat flux vector occurs in the fin of the membrane wall. Since heat can only be supplied from the higher temperature to the low temperature, the fin temperature must be higher than the temperature of the boiling water.

The alternate circuit diagram is described analytically by equation (1):

$$\vartheta_{fin} = \left(\frac{s}{\lambda}\right)_4 \cdot \dot{q} \cdot \frac{\left(\frac{s}{\lambda}\right)_5}{\left(\frac{s}{\lambda}\right)_3 + \left(\frac{s}{\lambda}\right)_4 + \left(\frac{s}{\lambda}\right)_5} + \vartheta_W \text{ resp. } \vartheta_{fin} = \dot{q} \cdot \left(\frac{s}{\lambda}\right)_{res} + \vartheta_W \qquad (1)$$

Equation (1) shows that the fin temperature can be represented as a linear function of the heat flux density for the case that the heat resistances of the wall construction and the temperature of the boiling water are known.

With this fundamental context it is now possible to use the measured temperature difference outside the boiler (ϑ_{fin}-ϑ_{vertex})[1] for the determination of the heat flux density.

Next, test facilities and constructions are presented, which allow for a validation of the above-mentioned online heat flux measuring technique and also the determination of small temperature differences on the outside of a membrane wall.

[1] The temperature difference between fin and vertex becomes in the following $\Delta\vartheta_{fin-vertex}$.

3 EXPERIMENTAL ARRANGEMENTS

3.1 Test Facility to Validate the Online Heat Flux Measurement

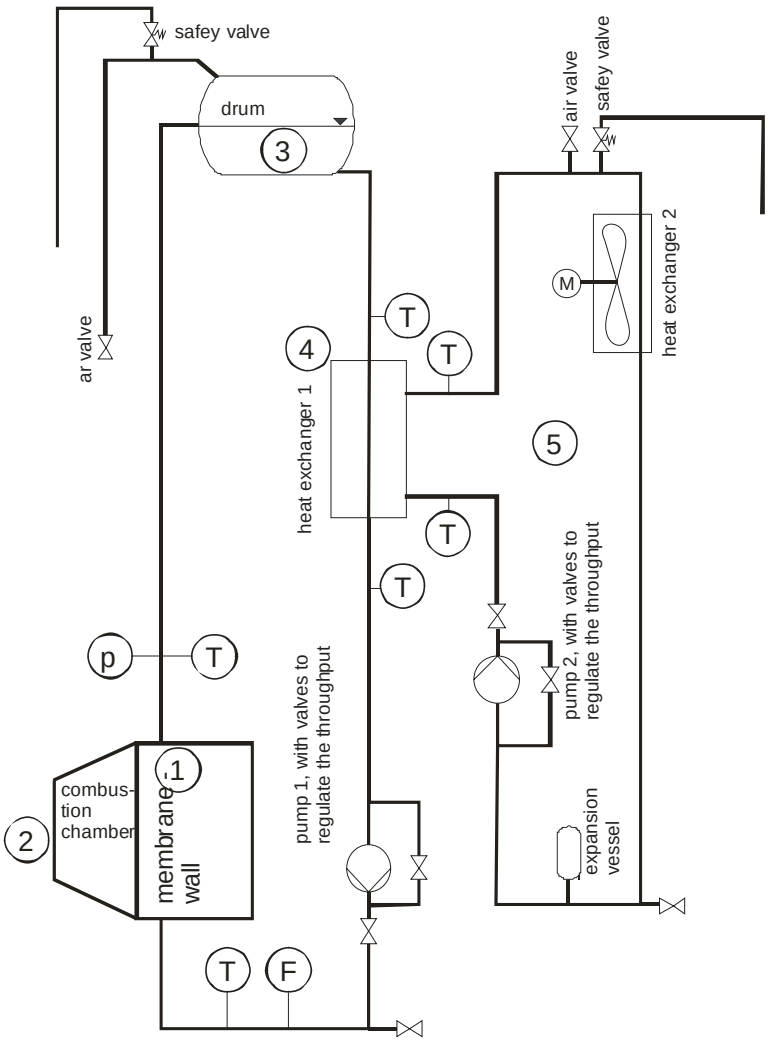

Fig. 2. Test facility, flow chart.

To validate the model of the temperature distribution on the outside of a membrane wall, which was presented in section 2, a test facility was constructed according to the flow chart shown in Fig. 2.

With help of this test facility, heat flux densities can be determined for different wall constructions (different refractory lining or deposits) by measuring the temperatures and mass flows of input and output of the membrane wall and balancing (refer to section 3.4). The temperature difference $\Delta\vartheta_{fin-vertex}$ is measured simultaneously.

The main components of the test facility are:

1. Membrane wall segment,
2. combustion chamber,
3. drum,
4. heat exchanger 1 / heating circuit,
5. heat exchanger 2 / cooling circuit.

No. 1 Membrane wall segment: The membrane wall segment consists of five tubes with a length of 500 mm and a fin pitch of 75 mm. On this membrane wall, different refractory materials or artificial deposit (fouling layers) can be positioned.

No. 2 Combustion Chamber: The heat flux is transferred to the membrane wall by a swivel-mounted combustion chamber which is equipped with two gas burners (maximum

throughput 8 kg/h). To distribute the heat flux density equally a copper plate with 50 mm thickness is positioned vertically in the combustion chamber.

Fig. 3. Combustion chamber with copper plate.

No. 3 Drum: The drum is connected to the membrane wall segment by a riser. The drum serves as a feed water reservoir and as a separator for the mixture of steam and water which is produced in the membrane wall.

No. 4 Heat exchanger 1 / heating circuit: The heat, which is supplied to the heating circuit by the membrane wall segment, is transmitted to the cooling circuit by an indirect heat exchanger.

No. 5 Heat exchanger 2 / cooling circuit: The heat release from the cooling circuit to the surroundings takes place in an air-cooled heat exchanger.

The test facility is equipped with measuring devices to determine the water temperatures in the inlet and outlet of the membrane wall segment, and the water throughput. By using this measuring data in an energy balance, the amount of energy supplied to the membrane wall segment can be calculated.

The measuring technique of detecting small temperature differences ($\Delta\vartheta_{fin\text{-}vertex}$) is presented separately in the following section.

3.2 Measuring Technique for Small Temperature Differences ($\Delta\vartheta_{fin\text{-}vertex}$)

As shown in section 2, a precise measurement of temperature differences on the outside of a membrane wall is essential for the online heat flux measurement. In this context, different methods and arrangements of measurements were investigated. Since detailed information was given in [2] about the different possibilities and installation variations, the currently implemented measuring technique and its validation are featured in this presentation.

The temperature difference $\Delta\vartheta_{fin\text{-}vertex}$ can by determined directly by spot-welded constantan (CuNi alloy) wires (direct use of the so-called thermoelectric effect). In contrast to a conventional NiCrNi-thermocouple, the thermoelectric potential will be generated between the base material (=membrane wall) and a constantan wire (refer to Fig. 4a).
The thermoelectric potential is generated only in the contact point of the constantan wire and the base material. If several constantan wires are welded to different points of the base material, for example to the fin and to the vertex of the tube - as shown in Fig. 4a -

thermoelectric potentials can be determined according to the temperature differences of the contact points of the constantan wires and the membrane wall.

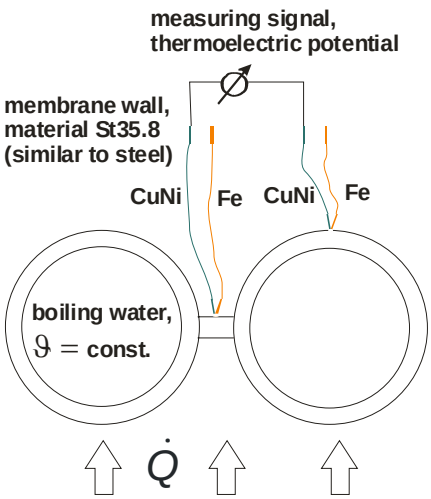

Fig. 4a. Principle of measurement.

Fig. 4b. Constantan wires on the outside of a membrane wall.

Fig. 4c. Spot-welded constantan wire.

To correlate the measured thermoelectric potential and the real temperature differences, the temperatures of the fin and the vertex of the membrane wall were determined with platinum temperature sensors (Pt-100-sensors) simultaneously.
Platinum temperature sensors show a high precision in the temperature range used here.
As the Pt-100-sensor is mounted to a material with a high thermal conductivity and the internal heat generation in the sensor is about 0.1 mW, the influence of the self-heating effect can be neglected.
For the practical application, the Pt-100-sensors are less suited for different reasons (e.g. difficulties with the electrical connection because of extremely thin wires, problems with the thermal contact between the sensor and the base material).
Figure 4b shows the arrangement of constantan wires on the back side of the membrane wall. A high number of measuring points were installed in order to examine whether the heat flux density is uniform over the investigated area or vary erratically.

3.3 Calibration of Temperature Difference Measurement System

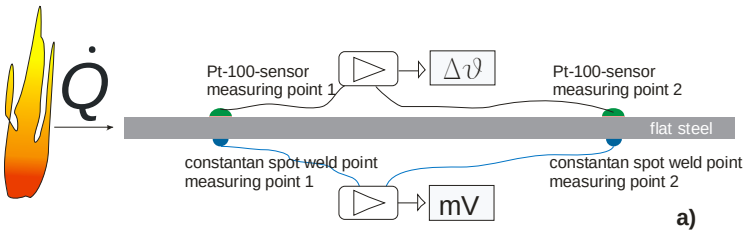

Fig. 5. Illustration of the experimental setup for the calibration of the thermoelectric potential.

Fig. 5 shows the experimental setup for the calibration of the measurement system. A Pt-100-sensor and a constantan wire are fixed on the opposite sides on flat steel plate. For the experiment, one side of the flat steel plate is heated up so that a temperature difference between the measuring points is generated.

The Pt-100-sensors and the constantan wires lie opposite to each other to ensure largely identical temperatures at the upper and the lower side of the plate. The temperature signals of the Pt-100-sensors at measuring point 1 and 2 (upper side), together with the signal of the thermoelectric potential between the constantan wires (lower side) are recorded simultaneously. The diagram in Fig. 6 shows their linear correlation between the measured temperature difference and the thermoelectric potential (calibration line). As the flat steel plate acts as one part of the thermocouple – in this experimental setup – it is obvious that it has to be made of boiler steel. During the experiment, both sides of the flat steel were heated up and cooled down in alternating order. Thus measuring point 1 can become warmer, respectively colder, than measuring point 2. For the thermoelectric potential between measuring point 1 and 2, this means the crossing of a zero point. The measuring signal of the thermoelectric potential (refer to Fig. 6) shows no discontinuity during the crossing of the zero point described above. This leads to the conclusion that the presented technique (refer to Fig. 4a) can be used for determining smallest temperature differences.

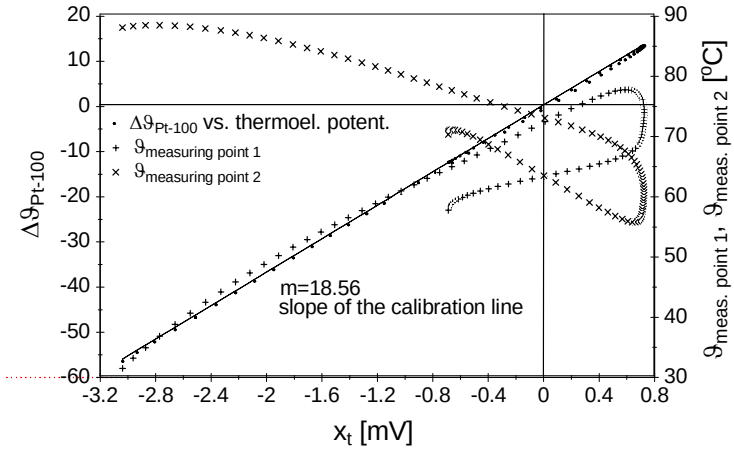

Fig. 6 Plot of the thermoelectric potential vs. the measured temperature difference.

Deviations of measuring points from the calibration line occur if the changes in temperature of one measuring point take place too fast. E.g. that even the tiny mass of the Pt-100-sensor and the spot-weld point (refer to Fig. 4c) can lead to a falsification of the calibration line during unsteady heating and cooling procedures.

3.4 Determination of the Heat Flux Density by Balancing

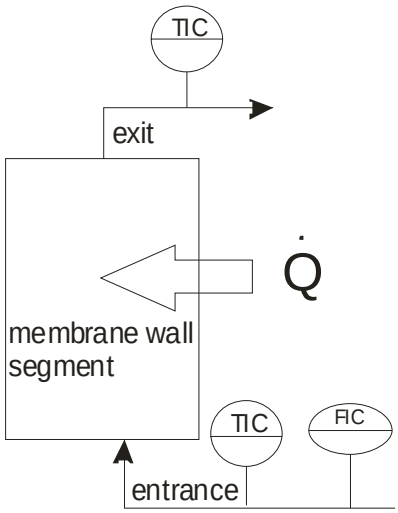

Fig. 7. Illustration of the validation system for the online heat flux measurement.

At the test facility (refer to Fig. 2), among other things, the water temperature at the entrance and the exit of the membrane wall segment and the water throughput are measured and recorded (refer to Fig. 7). From equation 2, the heat flux density supplied to the membrane wall segment can be calculated.

$$\dot{Q} = \rho_w \cdot \dot{V}_w \cdot c_w \cdot (T_{exit} - T_{entrance}) \qquad (2)$$

The throughput of water through the membrane wall segment is so high that the temperature difference between entrance and exit measures a few degrees. Consequently, the conditions in the membrane wall segment are close to the conditions in the real steam generator concerning the increase in temperature.

Fig. 8. JuSyS®SL-plate with holes to measure the temperature gradient.

3.5 Determination of the Heat Flux Density by Measuring Temperature Gradients in a Defined Material

By knowing the temperature gradient in a defined material, the specific heat flux can be calculated. Moreover, the surface temperature can also be calculated.

To measure the temperature gradient in the plate, 65 mm deep holes were drilled into the face (front) side of the JuSyS®SL plate (refer to Fig. 8). Ni-CrNi thermocouples were placed in these holes when the plate was mounted to the wall so that the temperatures could be measured during the experiments in a defined distance to each other.

4 MATHEMATICAL MODELLING OF THE HEAT FLUX DENSITY AND COMPARISON WITH EXPERIMENTAL RESULTS

As shown in section 2, specific temperature differences occur during operation at the backside of a membrane wall. This temperature difference depends on the design of the membrane wall and the heat flux density entering it.

Based on the boundary conditions of the test facility (refer to Fig. 2), a mathematical model was prepared with the FEM software FemLab [1]. With this model, the temperature profiles for a membrane wall lined with a mortar-fixed JuSyS®SL plate system was numerically simulated [3], [4].

Fig. 9 exemplifies the numerical simulation of the temperature profile for a JuSyS®SL refractory lining. In the numerical model, different thermal loads (heat flux densities) can be set. As a consequence of the specific heat flux – as already mentioned - a higher fin temperature occurs in comparison to the backside vertex of the tube.

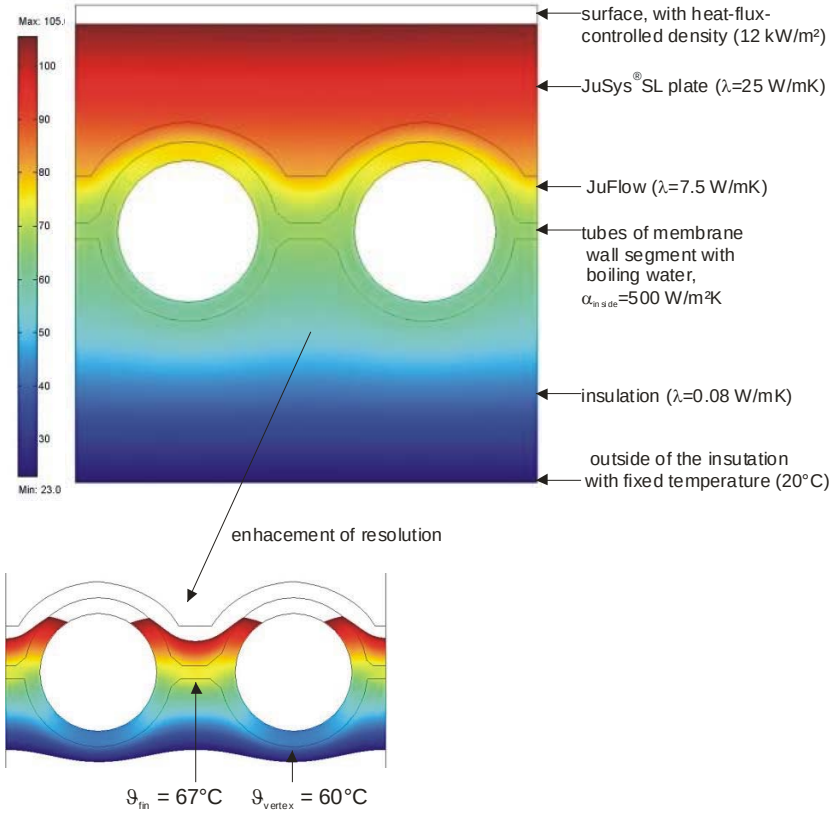

Fig. 9. FEM model.

By plotting the heat-flux-controlled density versus the calculated temperature difference between the fin and the vertex of the tube (refer to Fig. 10a), the linear correlation which was predicted by equation (1) can be found. The slope of the straight line is specific for a given wall design. The wall design involves different spacing and refractory lining or cladding and the heat transfer mechanism[2] at the inner side of the tubes of the membrane wall. The straight lines (correlation between the heat flux density and the temperature difference) calculated by the numerical model can be recognized as system characteristic lines. Thereby it is important that the system characteristic lines can still be used for a membrane wall lined with refractories even if deposits (fouling layers) occur on the surface of the refractory lining.

[2] In the tubes of the membrane wall of the test facility natural and forced convection occur. In the tubes of membrane walls of steam generators the convection is highly affected by bulk boiling.

From the experiments, system characteristic lines can also be obtained by balancing (see section 3.4).

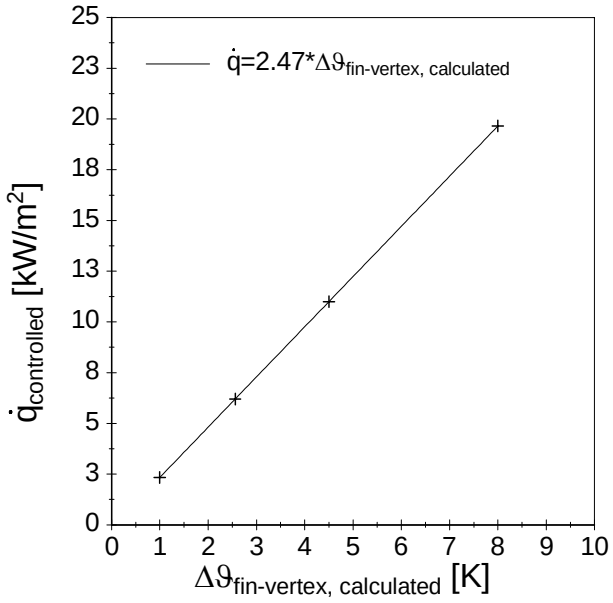

Fig. 10a. System characterization line for a JuSyS®SL system on the membrane wall segment obtained by the numerical simulation.

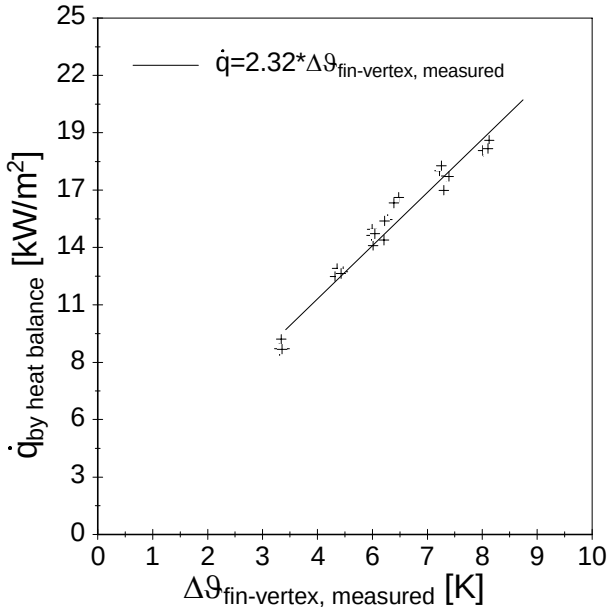

Fig. 10b. System characterization line for a JuSyS®SL system on the membrane wall segment obtained by energy balance.

Fig. 10b shows the heat flux density which was calculated by an energy balance versus the measured temperature differences *($\Delta\vartheta_{fin\text{-}vertex}$)*. In the diagram of Fig. 10b, the linear correlation between supplied heat flux density and measured temperature difference $\Delta\vartheta_{fin\text{-}vertex}$ can be recognized. The slopes of the system characteristic lines obtained from the numerical simulation (Fig. 10a) and obtained experimentally by using energy balance (Fig. 10b) are nearly equal. With the system characteristic line obtained by the numerical simulation and the measured temperature difference ($\Delta\vartheta_{fin\text{-}vertex}$) [3], the specific heat flux density can be determined.

A good correlation can be recognized by plotting the heat flux densities obtained by the system characterization line (from the numerical simulation) in combination with the measured temperature differences versus the heat flux densities obtained by the energy balance (Fig. 11a).

In the following the comparison between the heat flux density obtained by the energy balance (section 3.4) and the heat flux density obtained by the temperature gradient in a defined material (section 3.5) is discussed. Fig. 11b shows in analogy to Fig. 11a on the abscissa the heat flux density obtained by the energy balance and on the ordinate the heat

[3] The temperature differences ($\Delta\vartheta_{fin\text{-}vertex}$) can be calculated by the measured thermoelectric potential in combination with the calibration line (refer to Fig. 6).

flux density obtained by the measured temperature gradient in the wall. From Fig. 11b, it can be recognized and concluded that the measuring points deviate from the bisecting line. The heat flux densities obtained by the temperature gradients are lower than the heat flux densities obtained by the energy balance.

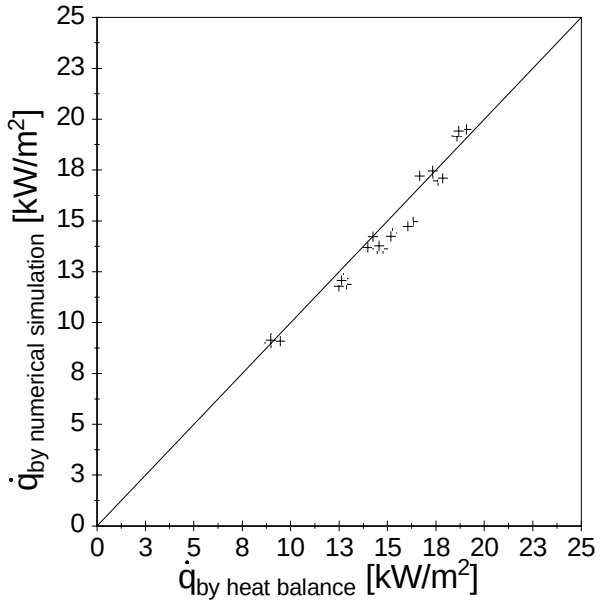

Fig. 11a. Heat flux density obtained by numerical calculation vs. heat flux density obtained by energy balance.

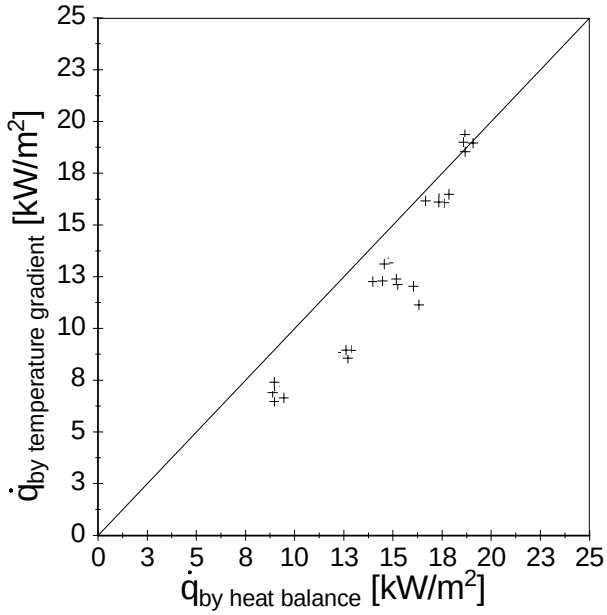

Fig. 11b. Heat flux density obtained by temperature gradient vs. heat flux density obtained by energy balance.

5 PRACTICAL APPLICATION

5.1 Installation of the Measuring Technique

Fig. 12a. Cut-out in the insulation of a boiler for installing the constantan wires.

On the membrane wall, outside of a steam generator, approximately 8 m above the secondary air nozzles constantan wire couples were spot-welded to five different measuring points. The front side (furnace side) of the membrane wall is lined with a *Karrelit* mix.

From the measuring point to the reference point in the signal amplifier the wires are made of constantan to avoid signal corruption.

The arrangement and numeration of the measuring points as well the dimensions are shown in Fig. 12b.

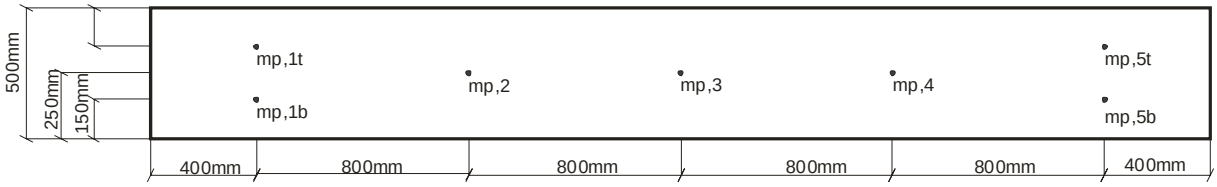

Fig. 12b. Arrangement and numeration of the measuring points on membrane wall of the boiler.

5.2 Measuring Results

The measurement data, which are presented and discussed in this section, were acquired during the start-up procedure of the boiler. The first part of the start-up procedure was carried out with process steam. The heating was continued with the oil burners of the boiler. In the following several characteristics of the measuring signals are discussed. The measurement signals are influenced either by operational factors (operational alterations) or system-caused fluctuations.

5.2.1 Operational Alteration

Fig. 13 shows the measuring signals of the measuring points 1 top (*mp,1t*), 3 (*mp,3*) and 5 top (*mp,5t*). The assignment of the measuring points to the individual position of installation is shown in Fig. 12b.

Before the ignition of the burners, the boiler was – as already mentioned – heated with process steam. In this state of operation, the fin of the membrane wall receives no heat

flux density from the boiler side as in standard operating conditions. The fins turn into ribs which deliver heat from the tube to the wall. Therefore, the fins have a lower temperature than the tubes. Consequently, the temperature difference ($\Delta\vartheta_{\text{fin-vertex}}$) becomes negative, i.e. the acquired signals have negative signs (refer to (1), Fig. 13a).

The ignition of the burners can be clearly noticed in Fig. 13a by the abrupt increase of the curves indicating the oil consumption *($\dot{V}_{burner\,1}$ and $\dot{V}_{burner\,2}$).* With the increasing oil consumption, the measuring signals for the temperature difference ($\Delta\vartheta_{\text{fin-vertex}}$) change sign. From this moment the fins of the membrane wall are at a higher temperatures than the tubes (refer to (2), Fig. 13a), because the wall receives a heat flux from the furnace side.

With the oil throughput remaining constant, it takes 4.5 hours for the measuring signals to become nearly constant (refer to (3), Fig. 13a). This effect results due to the change in heat supply. The heat supply changes from an internal heat source (heat from process steam in the tubes of the membrane wall) to an external heat source (heat from combustion from the side of the combustion chamber). Consequently, accumulation effects arise with a further heating-up of the entire wall (refractory lining, membrane wall and boiler water) (refer to (4), Fig. 13a). Due to the accumulation effects, the heating-up of the wall is to be seen as a transient process. Also the slow increase of the gas temperature in front of the super-heater (refer to (4), Fig. 13b) shows that the boiler is working in non-steady operating conditions.

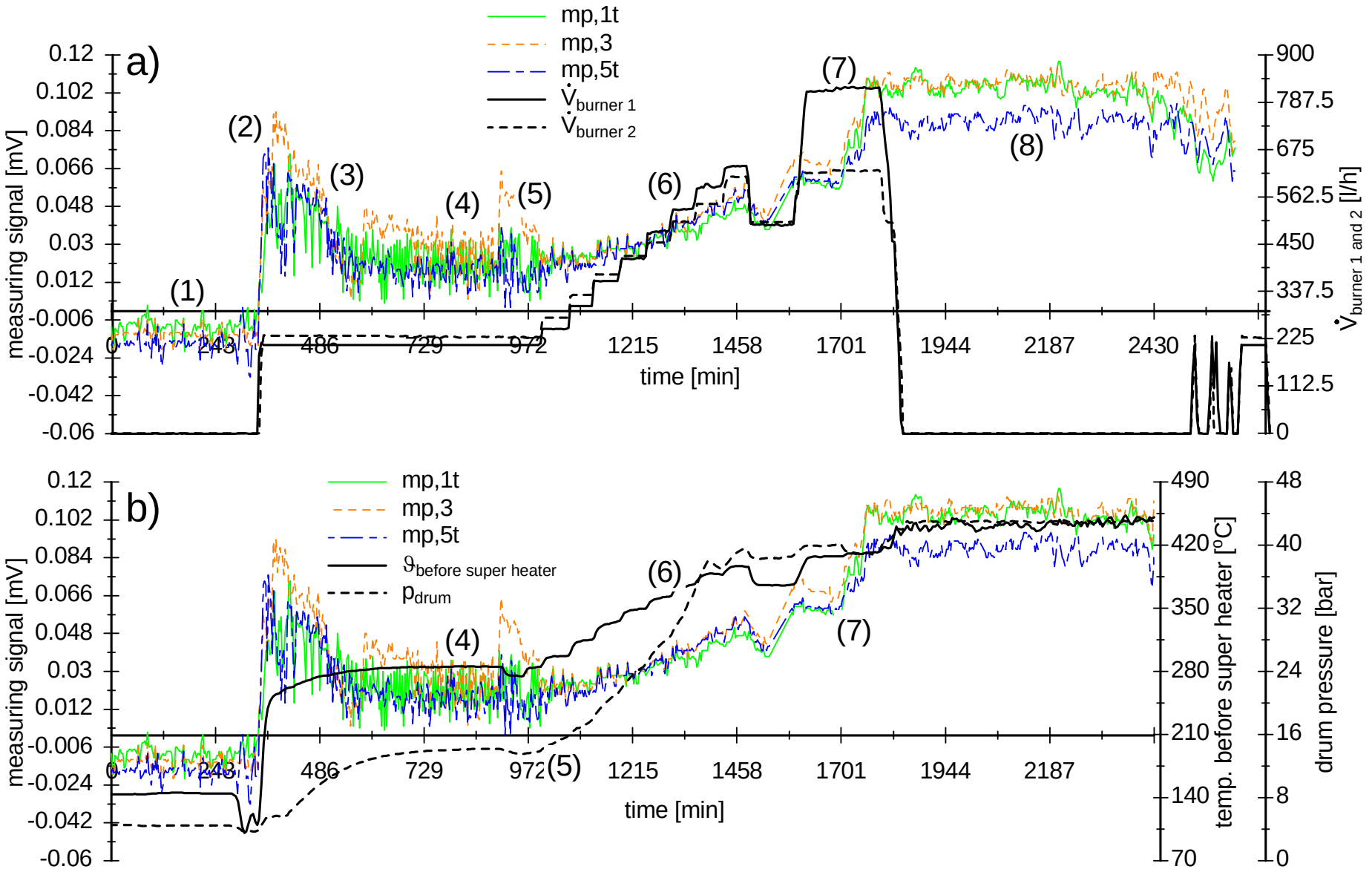

Fig. 13. Measuring signals – part 1.

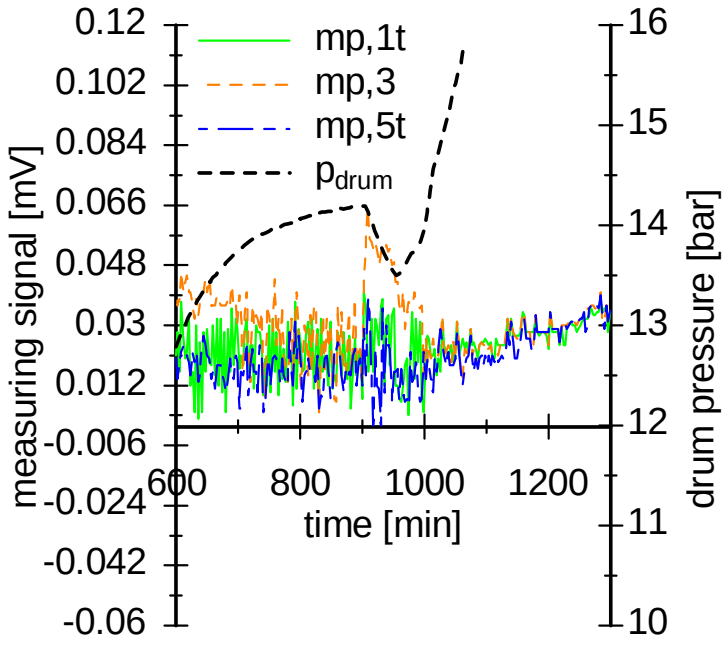

Fig. 14. Correlation between the drum pressure and the measuring signals.

At the time (5) (refer to Fig. 13a) a main valve in the water-steam circuit (in direction of the superheater) was opened which leads to a decrease of the system pressure indicated by the pressure of the drum. To clarify the correlation between the drum pressure (especially the decrease of the pressure) and the measuring signals, the relevant range is worked out on a larger scale (refer to Fig. 14). With a decrease of the pressure in the boiler system, certainly more steam is generated. Consequently, different temperatures and different heat transfer conditions occur in the tubes of the membrane wall. The fluctuations of the measuring signals in this period are probably caused by this non-steady process (refer to (5), *Fig. 13 and Fig. 14)*.

In the further course of the heating process of the boiler a distinct correlation between the increasing oil throughput, the gas temperature and the measuring signals can be seen (refer to (6), Fig. 13a).

During the second half of the full load oil throughput, the waste is charged to the boiler (refer to (7), Fig. 13a). Thus, the measuring signals increase clearly during the second half of the full load oil throughput (refer to (7), Fig. 13a and b). Hence a correlation between the oil throughput and the measuring signals can not be established anymore as the heat flux density delivered to the wall derives from the combustion of the oil and the waste.

5.2.2 System-caused Fluctuation

System-caused fluctuations are fluctuations in heat flux density caused by influences within the membrane wall system, e.g. different boiling modes or flow conditions in the tubes of the membrane wall. Reference should be made to the permanent difference of the measuring signals during the period of constant operating conditions (refer to (8), Fig. 13a). For the interpretation of these fluctuations, especially the measuring signals of nearby measuring points are taken into consideration.

Fig. 15 shows the measuring signals of the measuring points 1 top and bottom (*mp,1t; mp,1b*) and 5 top and bottom (*mp,5t; mp,5b*). The measuring points *mp,1t* and *mp1,b* are located 200 mm in vertical distance from each other. Fig. 15 shows that the measuring signals are nearly equal during the period the boiler is heated up with burners (refer to (1),

Fig. 15a). During the increase of the oil throughput the signals of the measuring points *mp,1t* and *mp,1b* start to drift apart (refer to (2), Fig. 15a). During the operation period of the boiler with waste, a remaining and more or less constant difference of the signals is noticed (refer to (3), Fig. 15a). The gas temperature before the super-heater and the drum pressure remain nearly constant during this period (refer to (3), Fig. 15b).

The signals of the measuring points *mp,5t* and *mp,5b* (vertical distance 200 mm from each other) show a similar behavior. But the signals of the measuring points *mp,5t* and *mp,5b* differ from each other during the heating-up period with process steam (refer to (4), Fig. 15b). During this period the signals show that at measuring point *mp,5b* more heat is delivered to the to membrane wall (signal of *mp,5b* is lower than signal of *mp,5t*). During normal operating conditions (refer to (3), Fig. 15b) measuring point *mp,5b* receives a higher heat flux density than measuring point *mp,5t* (signal of *mp,5b* is higher than the signal of *mp,5t*).

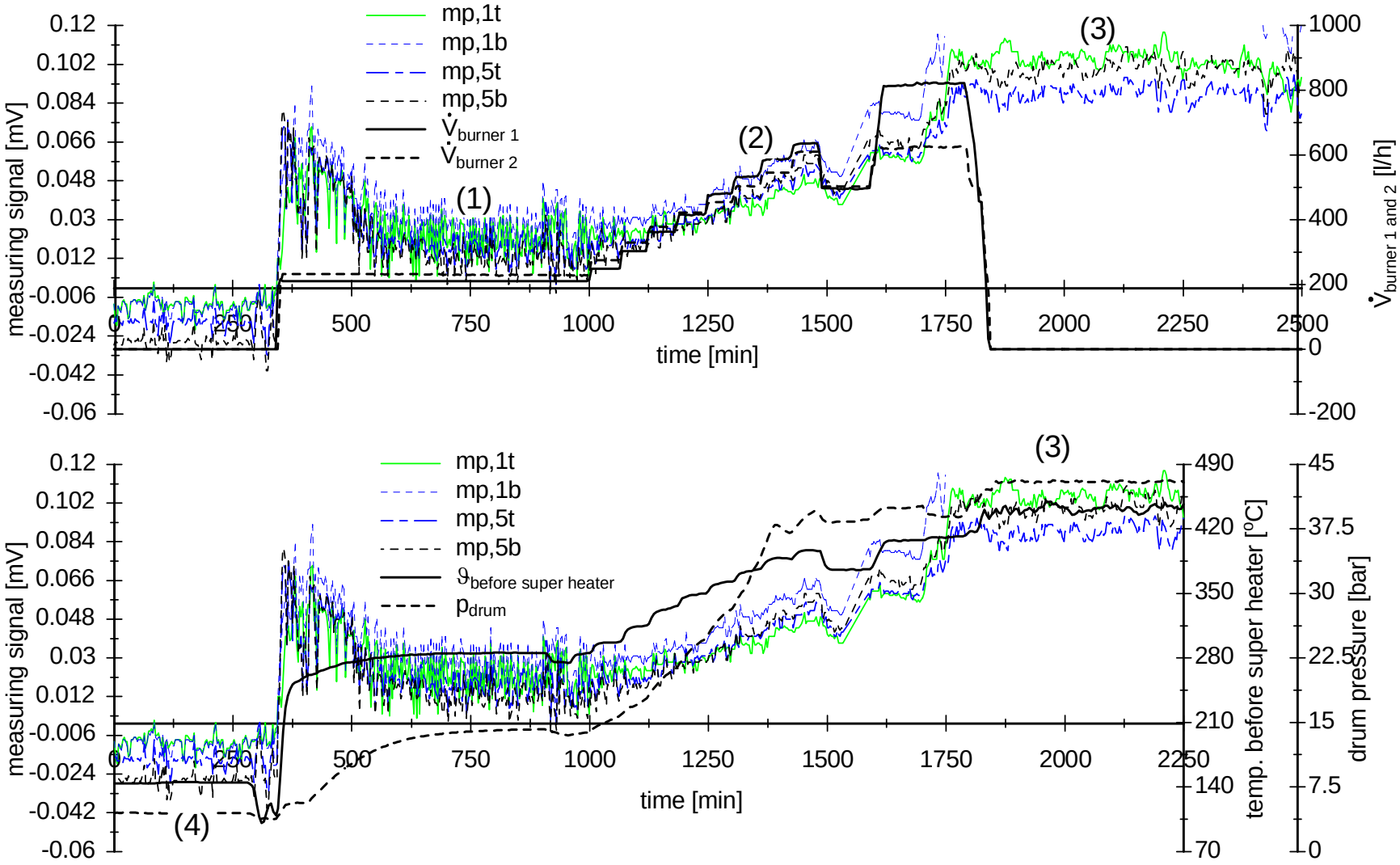

Fig. 15. Measuring signals – part 2.

In the following, an overview should be given that provides possible reasons for system-caused fluctuations.

- Different heat transfer conditions at the inside the boiler

  The investigated range and the distances between the measuring points are too small to obtain signal differences of up to 35% (compare signal from *mp,1t* and *mp,1b*; refer to (3), Fig. 15a).

- Constructive irregularities in the wall

  The refractory mix is placed on studded tubes of the membrane wall. These studs form a pattern as shown in Fig. 16. Consequently, different wall designs occur considering the cut section (refer to Fig. 16). If the wall design changes, the system characteristic lines also change (refer to section 4). The relation of the constantan wires, fixed to the backside of the membrane wall, to the studs on the furnace side of the wall, could not be estimated during the operation period of the boiler. To check whether the studs have an influence on the system characteristic line a 3D-FEM model was developed (refer to Fig. 16). Fig. 16 shows that there is no influence of the pattern of the fixed studs on the distribution of the temperature differences. Calculated temperatures of the fin are – as shown in Fig. 16 – the same in the cut section A and B (for a given heat flux density of 20 kW/m²).

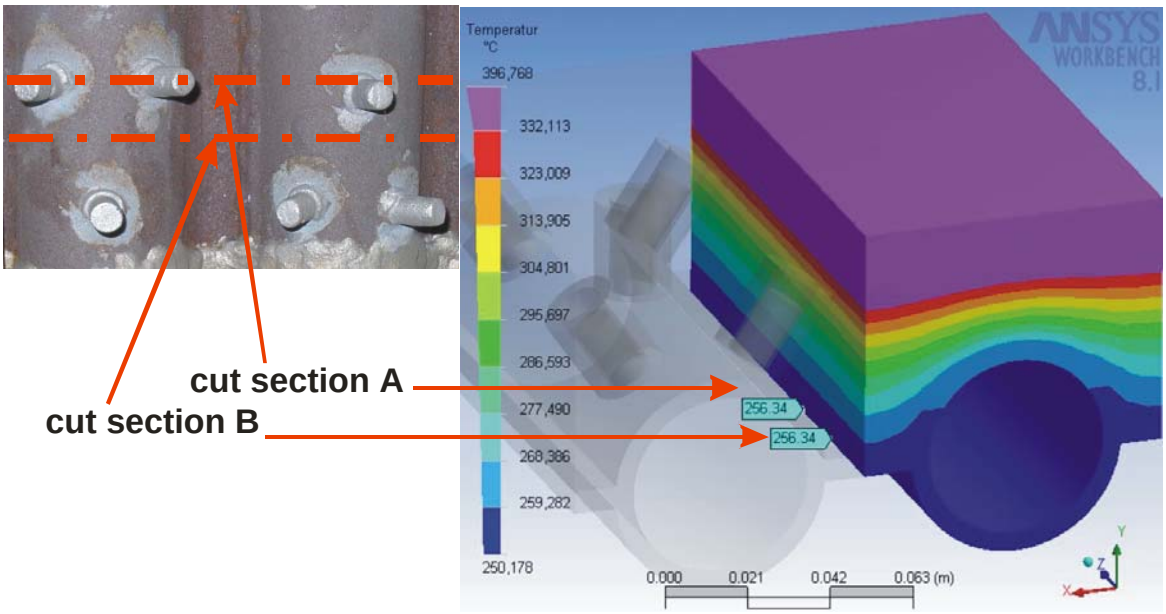

Fig. 16. 3D-Simulation of a membrane wall with a pitch of 80 mm, studded tubes.

Further, structural failures in the refractory mix (e.g. improper application) could be also a reason for system-caused fluctuations. These effects can cause a clear distortion of the temperature distribution in the membrane wall. Here, further investigations have to be carried out during the next maintenance period before continuing with numerical simulation.

- Heat flux dependent irregularities in the wall due to mechanical deformation

System-caused fluctuations can be further the result of heat flux dependent irregularities in the wall in case mechanical deformation in the refractory lining occurs during the operation period of the boiler. When the refractory lining is heated up, expansion of the material occurs due to thermal elongation. As the refractory lining has a higher temperature on the surface in comparison to the refractory material near the tubes of the membrane wall (during normal operating conditions) the refractory material can lift off (arch) the tubes [5]. Further quantification of the described effect has to be investigated on the test facility.

- Different boiling conditions in the tubes of the membrane wall.

  As already mentioned, system-caused fluctuations can occur due to different boiling conditions in the tubes of the membrane wall. Considering the design of the boiler tubes (different flow resistance due to bending of the tubes, e.g. for the secondary air nozzles) the water throughput in the tubes can differ from one tube to another one. Consequently, the boiling temperature of the water in tubes can also differ because of different pressures. For a further quantification of this effect more measurements have to be carried out.

6 Summary

The presented paper gives an overview concerning the state of development of a non invasive heat flux density measuring device. With the help of the temperature difference of the fin and the vertex at the membrane wall outside the steam generator heat flux densities can be detected. Using constantan wire couples, spot welded to the fin and vertex the detection of small temperature differences (approximately 0.1K) should be possible. First application of the measurement system in the industrial scale (MSWI-plant) show, a good sensitivity of the measurement signal (temperature difference respectively heat flux density). Investigations are necessary to determine operational alternations and system-caused fluctuations. Next to this it is necessary to investigate the relation of the heat flux density and formation of deposits, destruction of refractory tiles, corrosion etc. Further the heat flux density should be implemented as a signal for the online cleaning system.

Acknowledgement

We would like to thank the *Deutsche Bundesstiftung Umwelt (DBU)* for the financial support of the project *Development of a measuring system for online detection of heat flux density on membrane walls*.

7 APPENDIX

7.1 Symbols and abbreviations

Latin symbols			Greek symbols		
c	kJ/kgK	specific heat capacity	α	W/m²K	convective heat transfer coefficient
$\dot{q}$	kW/m²	heat flux density, specific heat flux	λ	W/mK	thermal conductivity
$\dot{Q}$	kW	heat flux, energy	ρ	kg/m³	density
R	Ω	thermal resistance	ϑ	°C	temperature
s	m	distance	Δ	-	difference
T	K	temperature			
$\dot{V}$	m³/s	vol. throughput			
x_T	[mV/°C]	thermoelectric potential			

Indices					
fin	-	fin of the membrane wall	v	-	vertex of the tubes
p	-	path	w	-	water
res	-	resulting			
s	-	surface			

7.2 Literature

[1] Beckmann, M.; Krüger, S: Online Heat Flux Measurement on Membrane Walls of Steam Generators of Municipal Solid Waste Incinerators, IT3 Conference, Houston, Texas, May 2005.

[2] Beckmann, M.; Krüger, S.; Spiegel, W.: Charakterisierung und messtechnischer Erfassung von betriebsspezifischen Wärmewiderständen an Membranwänden in Abfall und Biomasseverbrennungsanlagen. Erschienen in „Korrosionsforum 2“, Okt. 2005, Herausgeber: Born, M.;

[3] www.jg-refractoty-systems.com

[4] Martin, K., U.: Moderne Systeme zur Feuerfestauskleidung in Müllverbrennungen und Biomassekesseln - heutiger Stand der Technik. Uhlig-Symposium, Goslar, 10. / 11. Februar 2005.

[5] Krüger, J.: Thermische und mechanische Beanspruchung von Feuerfestmaterialien in Müllverbrennungsanlagen. Erschienen in Optimierung der Abfallverbrennung 1, Herausgeber, Thomé-Kozmiensky, K., J., März 2004, ISBN: 3-935317-16-6.